

Elastic Superhydrophobic and Photocatalytic Active Films Used as Blood Repellent Dressing

Jie Liu, Lijun Ye, Yuling Sun, Minghan Hu, Fei Chen, Seraphine Wegner, Volker Mailänder, Werner Steffen,* Michael Kappl, and Hans-Jürgen Butt*

Durable and biocompatible superhydrophobic surfaces are of significant potential use in biomedical applications. Here, a nonfluorinated, elastic, superhydrophobic film that can be used for medical wound dressings to enhance their hemostasis function is introduced. The film is formed by titanium dioxide nanoparticles, which are chemically crosslinked in a poly(dimethylsiloxane) (PDMS) matrix. The PDMS crosslinks result in large strain elasticity of the film, so that it conforms to deformations of the substrate. The photocatalytic activity of the titanium dioxide provides surfaces with both self-cleaning and antibacterial properties. Facile coating of conventional wound dressings is demonstrated with this composite film and then resulting improvement for hemostasis. High gas permeability and water repellency of the film will provide additional benefit for medical applications.

A well-known blood characteristic is its high propensity to thrombogenesis, i.e., the formation of blood clots when it comes into contact with foreign surfaces. This is due to the blood's intrinsic hemostatic mechanisms, induction of coagulation, and platelet activation.^[1] This coagulation effect inevitably results in the blood's strong adhesion to substrates, making it easily stick to surfaces. Blood coagulation can pose a serious side effect when it occurs on medical implants used in vivo, leading to a deterioration in the condition of the patient.^[2] Blood adhesion to surfaces such as clothes and wound dressings can cause contamination, waste, and even infections.^[3] In medical textiles, exposure and transfer of blood between patients and medical personnel during first-response care, or generally within hospitals, is of high concern, potentially causing bacterial or viral

infections.^[4] Therefore, developing efficient blood repellent surfaces is not only highly desirable but basically essential. Superhydrophobic surfaces have already been extensively investigated and applied in various fields, e.g., to improve heat transfer,^[5] in microfluidics,^[6] or to prevent icing.^[7] In recent studies, superhydrophobic surfaces have been reported to have great potential in repelling blood.^[8] The hierarchical structures with a trapped air plastron can effectively reduce the contact area between blood and surface and reduce platelet adhesion through hydrodynamic effects.^[8d] Paven et al. reported that a superamphiphobic membrane consisting of a fractal-like network of fluorinated silicon oxide nanospheres can resist blood adhesion.^[8b] However, practical application of superhydrophobic surfaces for blood repellency is still limited by poor chemical and mechanical stability and their lack of biocompatibility.

Ongoing regulations and concerns about using highly fluorinated substances have led to continuing research and development of substitutes for use in medical and other life science applications.^[4a]

In this study, we propose a method to prepare blood-repellent superhydrophobic surfaces by using hierarchical structures composed of biocompatible titanium dioxide (TiO₂) nanoparticles and poly(dimethylsiloxane) (PDMS).^[9] TiO₂ and PDMS are known as biocompatible materials because of which they have a broad application as implants.^[10] The PDMS provides surface hydrophobicity which is stable under UV illumination.^[11] The assembled nanoparticles lead to a rough nanostructure necessary for superhydrophobicity. Connecting them by the crosslinked PDMS results in elasticity and thus high stability under external forces. In addition, TiO₂ nanoparticles are photocatalytically active,^[12] making the surface to be antibacterial under UV-A illumination.^[13] Here, we demonstrate that this elastic, photocatalytic, superhydrophobic surface has excellent potential for usage as a blood repellent wound dressing.

As reported previously, PDMS can be easily grafted onto the surface of metal-oxide photocatalysts under the illumination of UV-A light.^[14] In order to graft (25–35% methylhydrosiloxane)-dimethylsiloxane copolymers (PDMS-copolymer, M_w : 1.9–2.0 kDa, Gelest Inc.) onto the surface of TiO₂ nanoparticles (diameter: 21 ± 5 nm, P25, Sigma), we dispersed bare particles (0.5 g) with the copolymer (30 mL) together in tetrahydrofuran (THF) via sonication for 1 h. After

Dr. J. Liu, L. Ye, Dr. Y. Sun, Dr. M. Hu, Dr. F. Chen, Prof. S. Wegner, Prof. V. Mailänder, Prof. W. Steffen, Dr. M. Kappl, Prof. H.-J. Butt
Max Planck Institute for Polymer Research
Ackermannweg 10, 55128 Mainz, Germany
E-mail: steffen@mpip-mainz.mpg.de; butt@mpip-mainz.mpg.de

Prof. V. Mailänder
Department of Dermatology
University Medical Center of the Johannes Gutenberg-University Mainz
Langenbeckstr. 1, 55131 Mainz, Germany

 The ORCID identification number(s) for the author(s) of this article can be found under <https://doi.org/10.1002/adma.201908008>.

© 2020 The Authors. Published by WILEY-VCH Verlag GmbH & Co. KGaA, Weinheim. This is an open access article under the terms of the Creative Commons Attribution License, which permits use, distribution and reproduction in any medium, provided the original work is properly cited.

DOI: 10.1002/adma.201908008

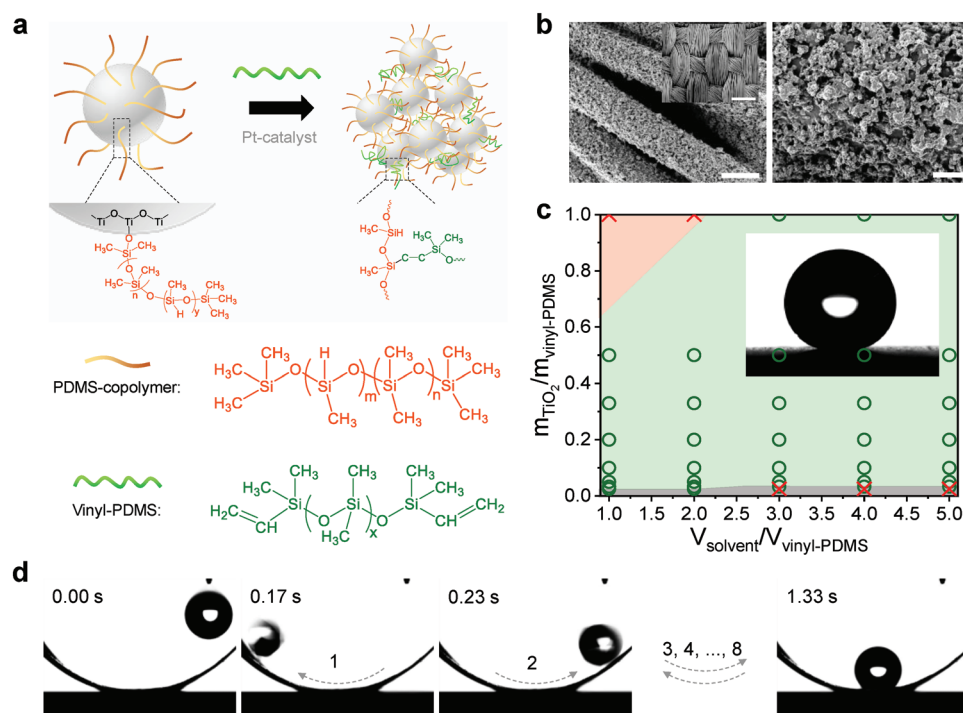


Figure 1. Superhydrophobic and photocatalytic active PDMS/TiO₂-films on different surfaces. a) Schemes illustrate fabrication of PDMS/TiO₂ from PDMS-copolymer modified TiO₂ nanoparticles and vinyl-PDMS. b) Morphology of polyester fabrics covered with crosslinked PDMS/TiO₂ film at different magnifications. From left to right, the scale bars are 10 μm (inset: 200 μm) and 2 μm . $m_{\text{TiO}_2}/m_{\text{vinyl-PDMS}} = 0.1$, $m_{\text{TiO}_2}/m_{\text{vinyl-PDMS}} = 3$, in which, $m_{\text{TiO}_2}/m_{\text{vinyl-PDMS}}$: mass ratio of modified TiO₂ nanoparticles to vinyl-PDMS; $V_{\text{solvent}}/V_{\text{vinyl-PDMS}}$: volume ratio of solvent to vinyl-PDMS. c) Parameters required to form superhydrophobic surfaces on the amount of modified TiO₂ particles, vinyl-PDMS, and solvent used for the preparation. ○: formation of superhydrophobic surfaces (light green background); ×: failed formation of superhydrophobic surface, which is the static contact angle for water was below 150° (pink and gray background). Inset shows the shape of a 5 μL water droplet on the PDMS/TiO₂ films. d) Sequence shows the periodical sliding of a water droplet (5 μL) on the bent polyurethane tape.

the THF was evaporated, the mixture was stirred and simultaneously illuminated by UV-A light (intensity: 5 mW cm^{-2}) for 8 h (Figures S1a and S2, Supporting Information). The modified TiO₂ nanoparticles quickly dispersed and were stable in toluene (Figure S1b, Supporting Information). The modified TiO₂ nanoparticles (dispersed in THF, 7.0 wt%) were mixed with vinyl-terminated PDMS (vinyl-PDMS, M_w : 62.0 kDa, Gelest) and Pt-catalyst (concentration relative to vinyl-PDMS: 0.005 wt%) with a certain ratio in solvent (toluene, THF or hexane). Using a Pt-catalyst, the $-\text{Si}-\text{H}$ bonds of PDMS-copolymers on modified particles react with the double carbon bond $-\text{CH}=\text{CH}_2$ of the vinyl-PDMS (Figure 1a),^[15] which drives the assembly and connection of particles by the vinyl-terminated PDMS with a covalent bond. Selected substrates, e.g., textiles, were immersed in the reacting mixture for 2 h at 60 °C after treating them with oxygen plasma. Afterward, PDMS residues and solvent were removed through rinsing in hexane. A superhydrophobic micro/nano-hierarchical structure of PDMS/TiO₂ film has formed on the chosen substrate.

Figure 1b shows the morphology of PDMS/TiO₂ film on polyester fabrics. The PDMS/TiO₂ film uniformly covers the textile surface, even the surfaces inside the fabrics. The static water contact angle on this surface was $\Theta = 165^\circ \pm 1^\circ$. The modified TiO₂ nanoparticles determined the formation of micro/nanostructures (Figures S3 and S4, Supporting Information). A surface prepared from unmodified TiO₂ nanoparticles has poor

water-repellent properties with advancing contact angles lower than 140°. The unmodified particles tend to aggregate in PDMS and as a result, the roughness of the films is not sufficient to allow for the formation of a superhydrophobic surface.^[16]

The amount of modified TiO₂ particles, vinyl-PDMS, and solvent used for the preparation determine whether superhydrophobic surfaces are obtained or not (Figure 1c). Here, we define surfaces to be superhydrophobic when their static contact angles exceed 150°. When using too high concentration of TiO₂ nanoparticles (pink part in Figure 1c, $m_{\text{TiO}_2}/m_{\text{vinyl-PDMS}} = 0.5$), the static contact angle of water on the PDMS/TiO₂ film was only around 142°. In contrast, when the particles and vinyl-PDMS are too diluted (gray part in Figure 1c, $m_{\text{TiO}_2}/m_{\text{vinyl-PDMS}} < 0.025$), no connective film forms. The low crosslink density between vinyl-PDMS and modified TiO₂ nanoparticles fails to connect particles. The static contact angle for water was below 150°. Therefore, in order to prepare superhydrophobic films, the contents of the components during fabrication should be in the range ($0.025 < m_{\text{TiO}_2}/m_{\text{vinyl-PDMS}} < 1$ and $1 < V_{\text{solvent}}/V_{\text{vinyl-PDMS}} < 5$) as indicated in green in Figure 1c.

As another example, we coated a polyurethane (PU) tape. After coating with a PDMS/TiO₂ film, the PU tape surface becomes superhydrophobic. To demonstrate the low energy dissipation of sliding drops, we bent the substrate and let a water drop slide periodically on the bent PU surface (Figure 1d and Movie S1, Supporting Information).

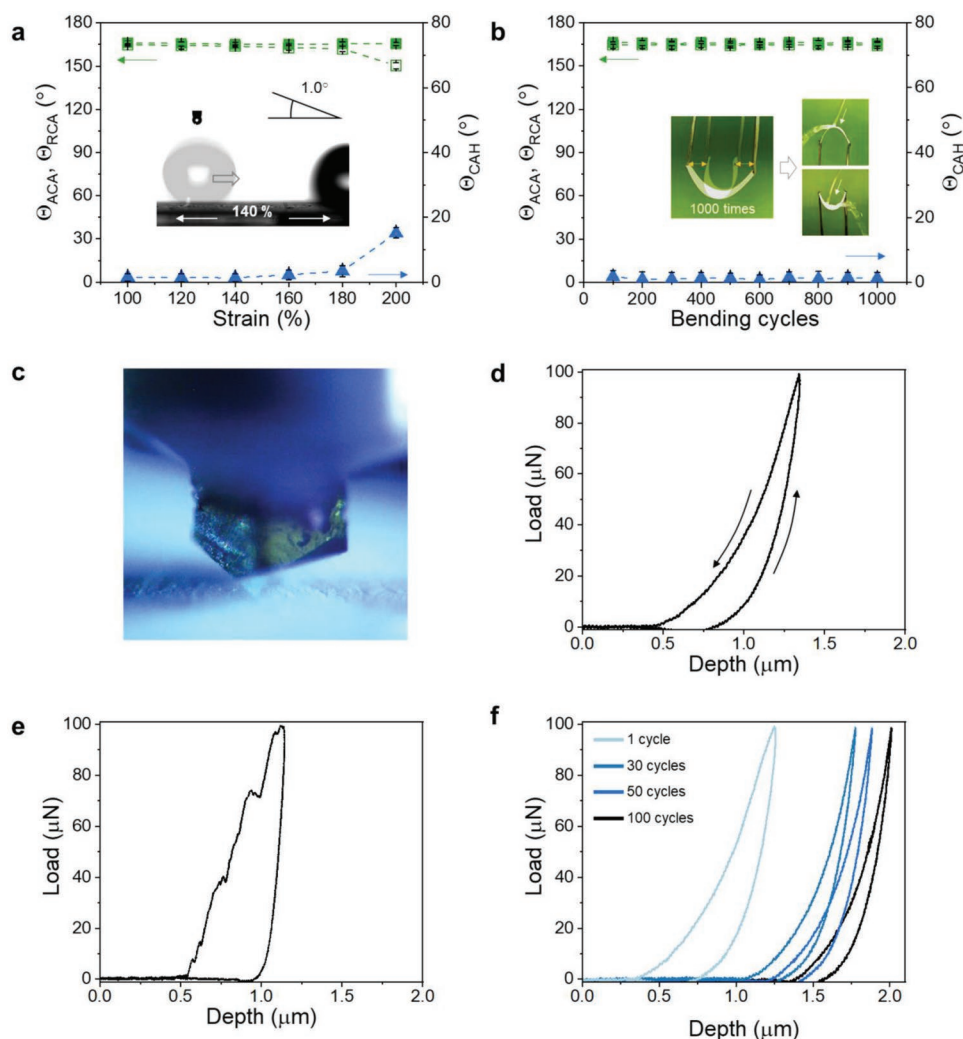


Figure 2. Mechanical stability of the PDMS/TiO₂ film. a) The advancing contact angle (Θ_{ACA} , ■), receding contact angles (Θ_{RCA} , □), and contact angle hysteresis (Θ_{CAH} , ▲) of the PDMS/TiO₂ film on PU tape as a function of strain. Inset shows sliding of a 5 μ L water drop on PDMS/TiO₂ film on a stretched (140% strain) and tilted (1°) polyurethane with PDMS/TiO₂ coating. b) The advancing contact angle (Θ_{ACA} , ■), receding contact angles (Θ_{RCA} , □), and contact angle hysteresis (Θ_{CAH} , ▲) of the PDMS/TiO₂ film on PU tape after repeated bending cycles. Inset images show the bending of the PDMS/TiO₂ film is carried out with bending angles ranging from 90° to 180° and the film maintains stable super-repelling to flowing water after 1000 bending cycles. c) Berkovich diamond indenter approaching the film surface. d) Indentation force versus depth curve as the indenter presses into and withdraws from the PDMS/TiO₂ film on a glass substrate. e) Indentation force versus depth curve as the indenter presses into and withdraws from the inorganic TiO₂ film. f) Indentation force versus depth curves for repeated indentation at one certain position.

A flat PU tape was used as a substrate to investigate the stability of the PDMS/TiO₂ film under stretching and bending conditions (Figure 2a,b). This is reflected by the variation of the advancing (Θ_{ACA}), receding (Θ_{RCA}) contact angles, and contact angle hysteresis ($\Theta_{ACA} - \Theta_{RCA}$). When the elongation of the film was smaller than 180%, the film exhibits superhydrophobicity, $\Theta_{ACA} = 166^\circ \pm 1^\circ$ and $\Theta_{RCA} = 165^\circ \pm 1^\circ$ with an extremely low contact angle hysteresis, $\Theta_{CAH} \approx 1^\circ$ (Figure 2a). A 5 μ L water droplet easily slides off the PDMS/TiO₂ PU surface stretched to 140% at a tilting angle of only 1°. Though the receding contact angle of the PDMS/TiO₂ film decreased to $150^\circ \pm 1^\circ$ after stretching to 200%, it is still superhydrophobic (Figure S5 and Movie S2, Supporting Information). In addition, Figure 2b shows that the PDMS/TiO₂ film has good resistance to bending, reflected by the stable advancing and receding contact

angles and low contact angle hysteresis after bending the surface between 90° and 180° for 1000 times. The PDMS/TiO₂ film also shows stable repellency to water flow in the bent state.

The elastic modulus and hardness of the material were measured by nanoindentation (Figure 2c–f). Figure 2d shows a typical indentation curve measured on the PDMS/TiO₂ film on a glass substrate. The hysteresis between approach and retract curves is due to partial plastic deformation of the sample during indentation. Indentation and unloading curves were smooth (Figure 2d), indicating that no cracking or disruptive failure occurred in the structure.

To elucidate the role of the PDMS for the elasticity of the film, we prepared an inorganic superhydrophobic surface by heating the PDMS/TiO₂ film at 500 °C for 30 min. This results in a TiO₂ film with similar surface structure, which could be rendered

superhydrophobic by treatment with a fluorosilane. Though the inorganic structure showed a higher modulus (574 MPa) and hardness (35 MPa) (Figure S6, Supporting Information) than PDMS/TiO₂ film (modulus: 90 MPa), its capability to respond elastically to large strain deformation was much lower than for the PDMS/TiO₂ film. Indentation curves of this inorganic film (Figure 2e) exhibited pronounced steps in the approach part. These steps indicate cracking or stepwise brittle failure of the structure and much less elastic recovery during retract with a larger permanent plastic deformation. In addition, for the PDMS/TiO₂ film, multiple test cycles of pressing and withdrawing indicated the good mechanical durability of the PDMS/TiO₂ film. Multiple loading curves at the same spot lead to the same smooth and continuous force lines (Figure 2f) indicating that no obvious cracking occurred even up to 100 cycles.

The PDMS/TiO₂ film possesses not only superhydrophobic but also photocatalytic properties and good UV stability. Even after UV-A illumination ($5 \pm 0.5 \text{ mW cm}^{-2}$) for 33 h, the advancing contact angle of the film was around $166^\circ \pm 1^\circ$ and the contact angle hysteresis $< 2^\circ$ (Figure 3a). This is attributed to the resistance of PDMS molecules to UV degradation. After contamination by oleic acid, the receding contact angle of the PDMS/TiO₂ film decreased from $165^\circ \pm 1^\circ$ to 0° but recovers after UV-A illumination ($5 \pm 0.5 \text{ mW cm}^{-2}$) for 2 h (Figure 3b). After six cycles of contamination using oleic acid and successive photodegradation, the PDMS/TiO₂ film remained superhydrophobic. Thus, PDMS/TiO₂ films possess self-cleaning properties under UV illumination that can deal with both physical (sand contamination, Figure S7, Supporting Information) and chemical contamination.

The PDMS/TiO₂ films are photocatalytically active and can degrade chemicals in solvents. As an example (Figure 3c), Nile red ($10 \mu\text{g mL}^{-1}$, 3 mL) dissolved in silicone oil (viscosity: 10 cSt) was degraded by PDMS/TiO₂ film in 5 h under the illumination of UV-A light ($5 \pm 0.5 \text{ mW cm}^{-2}$), which is much faster than that on just glass surface. The fluorescent intensity decreased when illuminating the sample with UV-A (Figure S8a, Supporting Information). Due to the low surface tension of silicone oil, the Nile red solution is in the Wenzel state on the film, where the dye molecules have direct contact with the TiO₂ nanoparticles.^[17] In contrast, an aqueous solution is in the Cassie state on the film—an air layer exists between solution and the film. As shown in Figure 3d, the UV-vis absorption spectrum shows that the Rhodamine B ($1 \mu\text{g mL}^{-1}$, 3 mL) in aqueous solution can be completely degraded in 4 h under UV-A illumination ($5 \pm 0.5 \text{ mW cm}^{-2}$), presenting the lighter color of the dye solution with longer UV-A illumination time (Figure S8b, Supporting Information).

The PDMS/TiO₂ films showed antibacterial properties (Figure 3e,f) under UV-A illumination. To demonstrate this, glass slides covered with PDMS/TiO₂ were placed at the bottom of an *E. coli* dispersion in fresh Lysogeny broth (LB)-ampicillin media (OD600 = 0.1) in sterile borosilicate 2-well plates. The bare glass slide was used as a control substrate. Giving the opacity of glass to UV light, a quartz slide (thickness: 170 μm) was used as a cap to inhibit liquid evaporation. The states (dead or live) of the *E. coli* on the glass and PDMS/TiO₂ film after incubation for 210 min under UV-A illumination ($5 \pm 0.5 \text{ mW cm}^{-2}$) and in the dark (Figure S9, Supporting Information) were

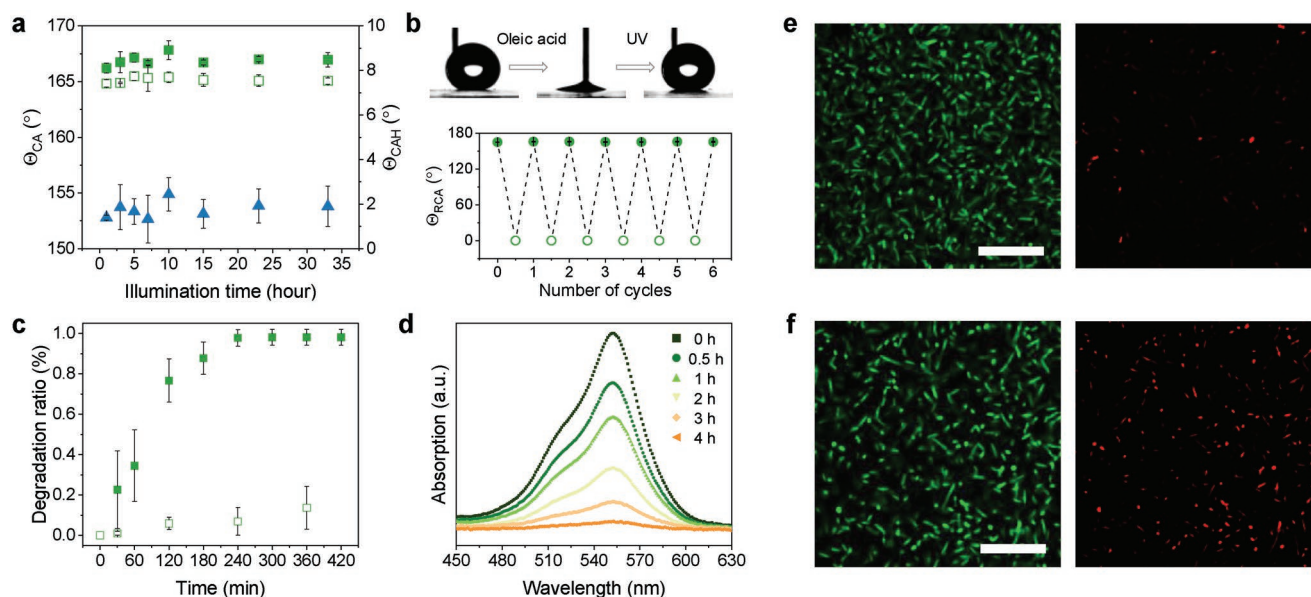


Figure 3. Photocatalytic activities of the PDMS/TiO₂ film ($m_{\text{TiO}_2}/m_{\text{vinyl-PDMS}} = 0.1$, $V_{\text{solvent}}/V_{\text{vinyl-PDMS}} = 3$). a) Advancing (Θ_{ACA} , ■) and receding contact angles (Θ_{RCA} , □) and contact angle hysteresis (Θ_{CAH} , ▲) of water on PDMS/TiO₂ film as functions of the UV-A illumination ($5 \pm 0.5 \text{ mW cm}^{-2}$) time. b) Images of the receding contact angle of water on the PDMS/TiO₂ film before (left), and after oleic acid contamination (middle), as well as after UV-A illumination for 2 h (right). The diagram shows the variation of the Θ_{RCA} of a water drop on the PDMS/TiO₂ film via oleic acid contamination and UV-A ($5 \pm 0.5 \text{ mW cm}^{-2}$) illumination for six cycles. c) Degradation ratio for Nile red over time under illumination with UV-A light ($10 \pm 1 \text{ mW cm}^{-2}$) in the presence of PDMS/TiO₂ film (■) and glass surface (□). $10 \mu\text{g mL}^{-1}$ of Nile red was dissolved in silicone oil (10 cSt). d) UV-vis spectra of Rhodamine B ($1 \mu\text{g mL}^{-1}$, 3 mL) aqueous solution after being degraded by PDMS/TiO₂ film for different times ($10 \pm 1 \text{ mW cm}^{-2}$). e, f) Confocal microscopy images of *E. coli* on the bare glass (e) and PDMS/TiO₂ film (f) after incubation for 210 min under UV-A illumination ($5 \pm 0.5 \text{ mW cm}^{-2}$). Green and red fluorescence indicate alive and dead *E. coli*, respectively. Scale bar: 20 μm .

studied using confocal microscopy. Green and red fluorescence respectively highlighted the live and dead *E. coli*. Bacteria incubated in the dark remain alive after 210 min (Figure S9, Supporting Information). In comparison, some of the *E. coli* bacteria are killed under UV illumination on both a bare glass surface and on PDMS/TiO₂ film. Compared to the bare glass (Figure 3e), significantly more bacteria are killed on the PDMS/TiO₂ film (Figure 3f), indicating additional antibacterial effect of the film beyond the direct action of UV-A. The TiO₂ nanoparticles on the film generate radicals when illuminated by UV light.^[14a,18] These radicals enhance the destruction of bacteria present on the PDMS film.

PDMS and TiO₂ are both biocompatible.^[19] Therefore, the PDMS/TiO₂ film can well be used to cover bleeding wounds. The common method for stopping bleeding is bandaging using a medical dressing which in general is hydrophilic. During bandaging, blood is lost by adsorption into the hydrophilic wound dressings. In contrast, blood repellent films prevent blood loss while stopping bleeding. However, the wetting property of blood on the surface is different from water because of the lower surface tension (56 mN m⁻¹) and its intrinsic hemostatic mechanisms.^[1,20] Our PDMS/TiO₂ film coated textile showed a static contact angle bigger than 150° for human blood without any pretreatment (Figure S10, Supporting Information) and a sliding angle of around 3° for a 20 μL blood droplet.

To further characterize the blood repellency, a 100 μL blood drop was allowed to evaporate on a coated textile for 1 h (Figure 4a–c). The size of the blood drop decreased (Figure 4a). After tilting the surface, the blood drop easily slid off from the surface tilted by 8° (Figure 4b, Movie S3, Supporting Information). No blood stain was left on the surface after removal of the drop (Figure 4c), no matter the platelets in blood were activated or not when exposed to the coated textile. Otherwise the blood drop would not easily slide on the textile. In another test we immersed the textile multiple times in blood. The contact angles of blood drops on coated textile did not change, demonstrating the stable blood repellent performance of our PDMS/TiO₂ coated textile (Figure 4d). The stable blood repellent performance of the coated textile attributes to the hybrid micro/nano-superhydrophobic structures supported by textile and the PDMS/TiO₂ film provides a stable air layer when exposed to blood (Figure 4e), thus blood presents a Cassie state on the surface. The intermittent nanostructures and air cushion greatly reduce the contact area between blood and surface. Furthermore, the small contact area reduces the adhesion area available to individual platelets hindering the hemostatic mechanisms.^[8d] Figure 4f shows that blood repellency of the PDMS/TiO₂ film modified wound dressing is still maintained when the film is stretched. There was no blood adhesion when flowing blood impacted onto wound dressing, even when it was stretched by 200%. The stability of the PDMS/TiO₂ films was further confirmed by a deformation test (Figure S11 and Movie S4, Supporting Information). After twisting the dressing tens of times, it still maintained its blood repellency.

For medical applications, the PDMS/TiO₂ film modified wound dressing exhibits several additional advantages. Blood leakage was prevented in the test bottle by using a PDMS/TiO₂ modified wound dressing (Figure 4g,h) for at least 3 h (Figure S12, Supporting Information). In contrast, the blood easily penetrated the unmodified wound dressing and thus entering

the water (Figure 4g and Movie S5, Supporting Information). A PDMS/TiO₂ modified wound dressing also prevented blood soaking the bandage in air (Figure 4h). The blocking effect of blood effectively reduces the loss of blood from a wound. In addition, the PDMS/TiO₂ film modified wound dressing offers good air permeability in a water environment. Figure 4i shows a strong reflection at the contact area of the film and the water indicates a distinctive interface on account of the superhydrophobicity of the film. At the same time, the air bubble, which was injected with a needle, was rapidly adsorbed by the film. Efficient air permeability provides sufficient oxygen to the wound and may promote healing.^[21]

Figure 4j,k shows an experimental simulation of a bleeding process. We cut a small incision into a polyvinyl chloride (PVC) tube to simulate a wound in a blood vessel. After pumping blood through the tube, “bleeding” took place. By fixing the tube on a forefinger and locating the incision at the finger joint, a wound was simulated. In contrast, with a continuously bleeding wound bandaged up with an unmodified wound dressing, the modified wound dressing efficiently stopped bleeding. Figure 4j shows that when the incision was bandaged by the PDMS/TiO₂ modified wound dressing, no bleeding was observed even if the joint of finger was bent. This is attributed to the high flexibility of the PDMS/TiO₂ film (Figure 4f). In contrast, bleeding continued when the incision was bandaged with an unmodified wound dressing (Figure 4k) and blood penetrated the wound dressing when the joint was bent.

In summary, a highly elastic, photocatalytic active, and superhydrophobic film was prepared by self-assembly of titanium dioxide nanoparticles driven by crosslinking reactions of PDMS. Substrates with different materials such as glass, PU, and polyester textiles can be easily modified with the film through immersion and heating at different intervals. Since the films are elastic up to high strains, they can adjust to stretching and bending of the support and they are mechanically robust. The photocatalytic activity of the film provides self-cleaning and antibacterial properties when exposed to UV-A light. Finally, it was shown that the coating we designed was able to enhance the hemostasis function of medical wound dressings. By using a PDMS/TiO₂ film, the wound dressing can effectively block leakage of blood while maintaining gas permeability even under water. Given these special properties, surfaces covered with this film will potentially combat contamination caused by blood adhesion and thus help to avoid infections transferred by blood.

Experimental Section

Modification of Titanium Dioxide Nanoparticles: 0.5 g titanium dioxide nanoparticles (TiO₂, diameter: 21 ± 5 nm, P25, Sigma) were dispersed in THF (10 mL) by sonication. 30 mL (25–35% methylhydrosiloxane)-dimethylsiloxane copolymer (PDMS-copolymer, M_w: 1.9–2.0 kDa, Gelest Inc.) was added and mixed uniformly with TiO₂ nanoparticles. The molecule structures are shown in Figure 1a. THF was evaporated for 24 h and the particle dispersion was illuminated with UV-A light (intensity: 10 mW cm⁻²) and stirred for 10 h.^[14a] After the reaction, the modified TiO₂ nanoparticles were purified by centrifugation at 10 000 rpm for 10 min and redispersed in THF. This process was repeated five times. The modified nanoparticles easily disperse in organic solvents such as toluene, THF, and hexane. The mass of modified TiO₂ nanoparticles dispersed in THF was measured by

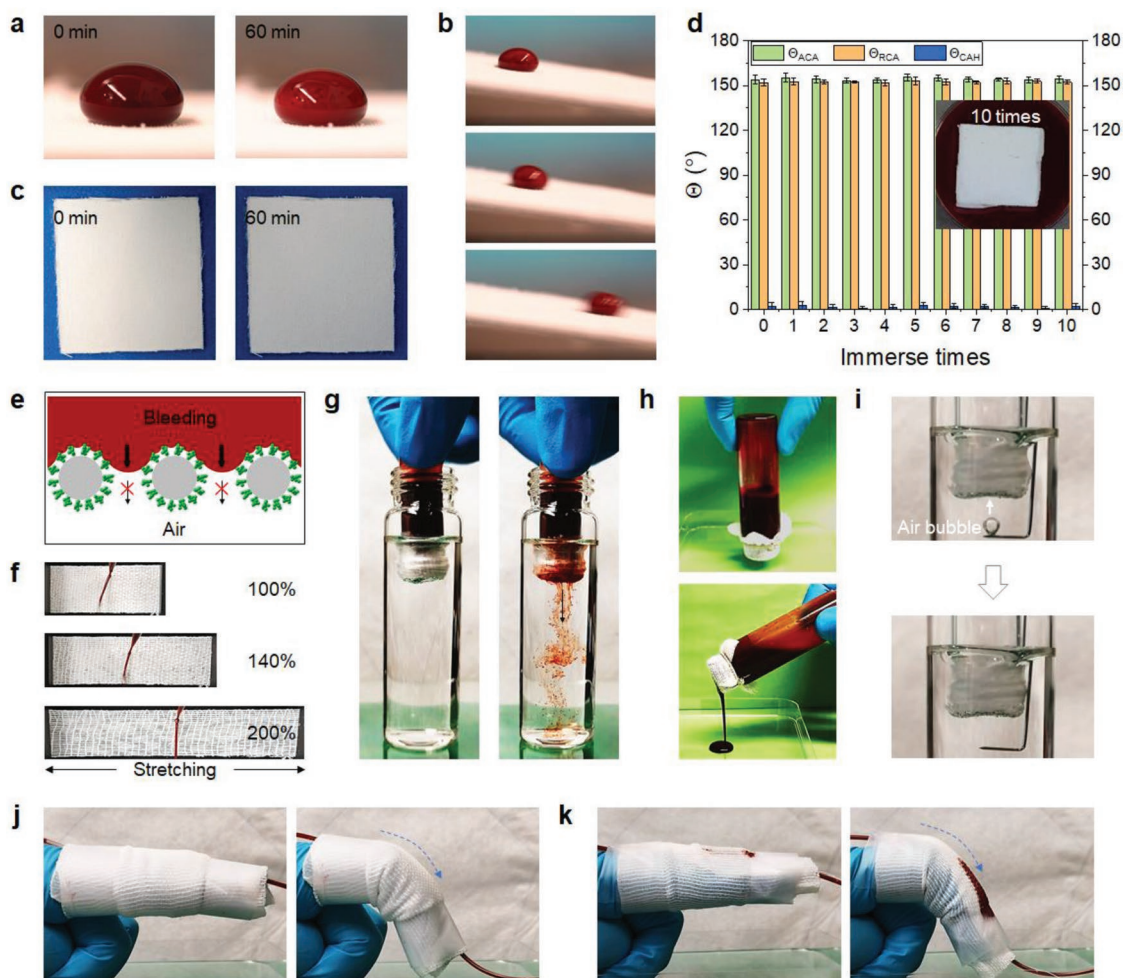


Figure 4. Hemostasis ability of wound dressing modified with the PDMS/TiO₂ film. a) Images of a 100 µL blood drop on PDMS/TiO₂ coated textile for 1 h. b) Sliding of blood drop (100 µL) after being located on the coated textile for 1 h. c) Photos of the coated textile before and after removal of the blood drop, the blood drop was located on the surface for 1 h. d) Advancing and receding contact angles of a sessile drop of human blood on a coated textile before and after immersing it one time for 1 h or multiple times in blood. The error derived from different measurements was estimated to be 3°. The contact angle difference was consistently 5°–6°. The experiments were carried out at room temperature (20 °C). e) Scheme illustrates the hybrid structure of the textiles covered with PDMS/TiO₂ film ($m_{\text{TiO}_2}/m_{\text{vinyl-PDMS}} = 0.1$, $V_{\text{solvent}}/V_{\text{vinyl-PDMS}} = 3$) hindering blood permeation. The gray circle: textile of the wound dressing; red part: blood; green part: PDMS/TiO₂ structure. f) Repellency of blood (red stripe) flowing on modified wound dressing at different elongations. g, h) Shielding ability of the modified wound dressing thus avoiding blood leakage into water (g) or air (h). i) Air permeability of the modified wound dressing under water. j, k) Simulated blocking of bleeding experiment. A poly(vinyl chloride) (PVC) tube is used to simulate the human blood vessel and a small incision is made simulating the wound. The arrows represent the direction of the blood flow in the tube.

weighing the deposition of 10 µL dispersion with a balance (Sartorius Genius ME, Mettler Toledo) after evaporation of THF. The concentration of particles was finally controlled to be 7.0 wt%.

Preparation of Highly Elastic Superhydrophobic and Photocatalytic Active Films: The modified TiO₂ nanoparticles (dispersed in THF, 7.0 wt%) were mixed with the vinyl-terminated PDMS (vinyl-PDMS, M_w : 62.0 kDa, Gelest) as well as Pt-catalyst (0.005 wt% relative to vinyl-PDMS, platinum(0)-1,3-divinyl-1,1,3,3-tetramethyldisiloxane complex solution in xylene, Gelest) at a certain ratio in solvent toluene. The substrates (glass, polyester fabrics, polyurethane, commercial wound dressings) were modified to be superhydrophilic with oxygen plasma (5 min, power: 100%). Then the substrates were immersed in the mixture and it was allowed to react for 6 h at 60 °C in a closed chamber. The crosslinking reaction between PDMS molecules occurred both in bulk and on the substrates' surfaces and formed gel. After washing the samples with toluene to remove PDMS residues, superhydrophobic nanostructures formed on the surface.

Measurement of the Mechanical Property of the Film: An MFP-3D nanoindenter (Asylum Research, Santa Barbara, CA, USA) equipped with a diamond Berkovich indenter was used. A maximum loading force of 100 µN was applied. Young's modulus and hardness of the structures were extracted from the indentation curves by fitting the unloading curves with the Oliver–Pharr model.

Bacterial Cell Viability Assay: *E. coli* K12 MG1655 were transformed with a fluorescent protein expression plasmid (GFP-pTrc99A, ampicillin resistant, isopropyl β-D-thiogalactoside (IPTG) inducible). 10 mL of LB medium containing 50 µg mL⁻¹ ampicillin and 0.5×10^{-3} M IPTG were inoculated with a single colony and incubated overnight at 37 °C at 250 rpm. The bacteria were diluted with phosphate buffer saline (PBS), or LB medium, to the desired density ($OD_{600} = 0.1$). The glass slides (control) and PDMS/TiO₂ film-covered glass slides were fixed on the bottom of sterile borosilicate 2-well plates (ibidi µ-Slide, glass bottom). 2 mL of bacterial solution was added and incubated for up to 210 min in the dark and under UV-light irradiation (5 ± 0.5 mW cm⁻²),

respectively. To determine the bacterial viability after incubation with the sample surfaces, the bacteria were mixed with propidium iodide (PI, 1 $\mu\text{L mL}^{-1}$ bacterial culture), which selectively enters cells with damaged membranes and incubated for 15 min in order to stain the dead cells. Stained bacteria were observed using a Leica SP8 laser scanning confocal microscope with excitation wavelengths of 488 and 610 nm. All bacteria display green fluorescence due to the expression of the GFP protein. Dead bacteria display red fluorescence of PI.

Blood Repellency Test: A 100 μL human blood drop was added on the modified textile and waited for 1 h. After tilting the surface, the blood drop easily slides off from the surface tilted for 8°. For another stability test, the coated textile was immersed into human blood for one to ten times, every time the surface was immersed for 1 h. The advancing and receding contact angles as well as contact angle hysteresis were measured. The experiments were carried out at room temperature (20 °C). Human blood was obtained from the Department of Transfusion Medicine Mainz from ten healthy donors after physical examination and after obtaining their informed consent in accordance with the Declaration of Helsinki. The use of human blood was approved by the local ethics committee “Landesärztekammer Rheinland-Pfalz” (837.439.12 (8540-F)).

Hemostasis Experiment: The PDMS/TiO₂ layer was laid on the commercial stretchable wound dressing. A PVC tube was used to simulate a blood vessel. An incision was cut into the tube to simulate a wound. The PVC tube was fixed on a forefinger with the incision site located at the finger joint, simulating the state of a wound near a joint. Experiments were conducted with the incision being respectively covered by layers of modified (three layers) or unmodified (three layers) wound dressing. The hemostasis effect of the wound dressing was observed after adding human blood into the tube during which the forefinger was bent.

Supporting Information

Supporting Information is available from the Wiley Online Library or from the author.

Acknowledgements

The authors are grateful for the financial support from the ERC advanced grant 340391 SUPRO (H.-J.B.). The authors would like to express their gratitude to Prof. Sanghyuk Wooh for his fruitful suggestions.

Conflict of Interest

The authors declare no conflict of interest.

Author Contributions

J.L. designed and performed research. J.L., L.Y., Y.S., M.H., F.C., S.W., V.M., W.S., M.K., and H.-J.B. contributed new reagents/analytic tools. J.L. and Y.S. analyzed data. J.L., W.S., M.K., and H.-J.B. wrote the paper. All authors have given approval to the final version of the paper.

Keywords

blood repellent materials, dressings, photocatalysis, superhydrophobicity

Received: December 6, 2019
Revised: December 31, 2019
Published online: February 3, 2020

- [1] a) A. C. Lima, J. F. Mano, *Nanomedicine* **2015**, *10*, 103; b) A. C. Lima, J. F. Mano, *Nanomedicine* **2015**, *10*, 271.
- [2] a) J. M. Nokes, R. Liedert, M. Y. Kim, A. Siddiqui, M. Chu, E. K. Lee, M. Khine, *Adv. Healthcare Mater.* **2016**, *5*, 593; b) C. Barras, K. Myers, *Eur. J. Vasc. Endovasc.* **2000**, *19*, 564; c) D. Stoeckel, A. Pelton, T. Duerig, *Eur. Radiol.* **2004**, *14*, 292; d) M. Wong, F. Cheng, H. Man, *Appl. Surf. Sci.* **2007**, *253*, 7527; e) S. Shabalovskaya, J. Anderegg, J. Van Humbeeck, *Acta Biomater.* **2008**, *4*, 447.
- [3] a) E. J. Quebbeman, G. L. Telford, S. Hubbard, K. Wadsworth, B. Hardman, H. Goodman, M. S. Gottlieb, *Ann. Surg.* **1991**, *214*, 614; b) E. M. Beltrami, I. T. Williams, C. N. Shapiro, M. E. Chamberland, *Clin. Microbiol. Rev.* **2000**, *13*, 385; c) J. R. Hall, *Anesth. Analg.* **1994**, *78*, 1136; d) M. Torabinejad, R. K. Higa, D. J. McKendry, T. R. P. Ford, *J. Endod.* **1994**, *20*, 159.
- [4] a) S. Schellenberger, P. J. Hill, O. Levenstam, P. Gillgard, I. T. Cousins, M. Taylor, R. S. Blackburn, *J. Cleaner Prod.* **2019**, *217*, 134; b) V. K. Midha, A. Dakuri, V. Midha, *J. Ind. Text.* **2013**, *43*, 174; c) R. K. Virk, G. N. Ramaswamy, M. Bourham, B. L. Bures, *Text. Res. J.* **2004**, *74*, 1073.
- [5] a) Y. Hou, M. Yu, X. Chen, Z. Wang, S. Yao, *ACS Nano* **2014**, *9*, 71; b) C. S. Sharma, J. Combe, M. Giger, T. Emmerich, D. Poulikakos, *ACS Nano* **2017**, *11*, 1673.
- [6] a) C. Liu, J. Ju, Y. Zheng, L. Jiang, *ACS Nano* **2014**, *8*, 1321; b) J. Liu, H. Guo, B. Zhang, S. Qiao, M. Shao, X. Zhang, X. Q. Feng, Q. Li, Y. Song, L. Jiang, J. Wang, *Angew. Chem., Int. Ed.* **2016**, *55*, 4265.
- [7] a) Q. Zhang, M. He, J. Chen, J. Wang, Y. Song, L. Jiang, *Chem. Commun.* **2013**, *49*, 4516; b) P. Guo, Y. Zheng, M. Wen, C. Song, Y. Lin, L. Jiang, *Adv. Mater.* **2012**, *24*, 2642.
- [8] a) S. Moradi, N. Hadesfandiari, S. F. Toosi, J. N. Kizhakkedathu, S. G. Hatzikiriakos, *ACS Appl. Mater. Interfaces* **2016**, *8*, 17631; b) M. Paven, P. Papadopoulos, S. Schottler, X. Deng, V. Mailander, D. Vollmer, H. J. Butt, *Nat. Commun.* **2013**, *4*, 2512; c) S. Movafaghi, V. Leszczak, W. Wang, J. A. Sorkin, L. P. Dasi, K. C. Popat, A. K. Kota, *Adv. Healthcare Mater.* **2017**, *6*, 1600717; d) V. Jokinen, E. Kankuri, S. Hoshian, S. Franssila, R. H. A. Ras, *Adv. Mater.* **2018**, *30*, 1705104; e) T. Zhu, J. Wu, N. Zhao, C. Cai, Z. Qian, F. Si, H. Luo, J. Guo, X. Lai, L. Shao, J. Xu, *Adv. Healthcare Mater.* **2018**, *7*, 1701086; f) Q. Wei, C. Schlaich, S. Prevost, A. Schulz, C. Bottcher, M. Gradzielski, Z. H. Qi, R. Haag, C. A. Schalley, *Adv. Mater.* **2014**, *26*, 7358.
- [9] a) C. Cui, H. Liu, Y. Li, J. Sun, R. Wang, S. Liu, A. L. Greer, *Mater. Lett.* **2005**, *59*, 3144; b) M. Khorasani, H. Mirzadeh, P. Sammes, *Radiat. Phys. Chem.* **1999**, *55*, 685.
- [10] a) A. Dalu, B. S. Blaydes, L. G. Lomax, K. B. Delclos, *Biomaterials* **2000**, *21*, 1947; b) A. Daniels, *Swiss Med. Wkly.* **2012**, *142*, w13614; c) K. Shiraiishi, H. Koseki, T. Tsurumoto, K. Baba, M. Naito, K. Nakayama, H. Shindo, *Surf. Interface Anal.* **2009**, *41*, 17; d) M. Ma, M. Kazemzadeh-Narbat, Y. Hui, S. Lu, C. Ding, D. D. Chen, R. E. Hancock, R. Wang, *J. Biomed. Mater. Res., Part A* **2012**, *100*, 278.
- [11] a) B. Cortese, S. D'Amone, M. Manca, I. Viola, R. Cingolani, G. Gigli, *Langmuir* **2008**, *24*, 2712; b) M. Jin, X. Feng, J. Xi, J. Zhai, K. Cho, L. Feng, L. Jiang, *Macromol. Rapid Commun.* **2005**, *26*, 1805.
- [12] A. Fujishima, T. N. Rao, D. A. Tryk, *J. Photochem. Photobiol., C* **2000**, *1*, 1.
- [13] Z. Huang, P.-C. Maness, D. M. Blake, E. J. Wolfrum, S. L. Smolinski, W. A. Jacoby, *J. Photochem. Photobiol., A* **2000**, *130*, 163.
- [14] a) S. Wooh, N. Encinas, D. Vollmer, H.-J. Butt, *Adv. Mater.* **2017**, *29*, 1604637; b) S. Wooh, H. J. Butt, *Angew. Chem., Int. Ed.* **2017**, *56*, 4965.
- [15] D. F. Cheng, C. Urata, M. Yagihashi, A. Hozumi, *Angew. Chem., Int. Ed.* **2012**, *51*, 2956.

- [16] J. V. I. Timonen, M. Latikka, O. Ikkala, R. H. A. Ras, *Nat. Commun.* **2013**, *4*, 2398.
- [17] R. N. Wenzel, *Ind. Eng. Chem.* **1936**, *28*, 988.
- [18] a) X. Sheng, Z. Liu, R. Zeng, L. Chen, X. Feng, L. Jiang, *J. Am. Chem. Soc.* **2017**, *139*, 12402; b) J. Li, G. Chen, Y. Zhu, Z. Liang, A. Pei, C.-L. Wu, H. Wang, H. R. Lee, K. Liu, S. Chu, Y. Cui, *Nat. Catal.* **2018**, *1*, 592.
- [19] a) S. L. Peterson, A. McDonald, P. L. Gourley, D. Y. Sasaki, *J. Biomed. Mater. Res., Part A* **2005**, *72A*, 10; b) Y. Wang, C. Wen, P. Hodgson, Y. Li, *J. Biomed. Mater. Res., Part A* **2014**, *102*, 743.
- [20] a) E. Hrnčič, J. Rosina, *Physiol. Res.* **1997**, *46*, 319; b) J. Rosina, E. Kvasnak, D. Suta, H. Kolarova, J. Malek, L. Krajci, *Physiol. Res.* **2007**, *56*, S93.
- [21] G. M. Gordillo, C. K. Sen, *Am. J. Surg.* **2003**, *186*, 259.